Preparation of Highly Dispersed Pentlandites $(M,M')_9S_8$ (M, M′ = Fe, Co, Ni) and Their Catalytic Properties in Hydrodesulfurization

Igor Bezverkhyy,* Pavel Afanasiev,‡ and Michel Danot†

Institut de Recherches sur la Catalyse, 2 avenue A. Einstein, 69626 Villeurbanne Cedex, France and Institut des Matériaux Jean Rouxel, UMR 6502, CNRS-University Nantes, BP 32229, 2, rue de la Houssinière, 44322 Nantes Cedex 3, France

Received: January 21, 2004; In Final Form: March 22, 2004

A series of highly dispersed single phase pentlandites (Co_9S_8, $NiCo_8S_8$, $FeCo_8S_8$, $Ni_3Co_6S_8$, $Ni_{4.5}Fe_{4.5}S_8$) was prepared by coprecipitation followed by sulfidation and reducing treatment at 300 °C. These mixed sulfides consist of crystalline particles with homogeneous distribution of the elements as shown by high-resolution microscopy and EDX analysis. The distribution of the cations in tetrahedral and octahedral sites of the pentlandite structure was characterized by EXAFS and Mössbauer spectroscopy. The catalytic activity of the sulfides in the model thiophene hydrodesulfurization reaction increases in the following order: $Ni_{4.5}Fe_{4.5}S_8 \ll FeCo_8S_8 < Co_9S_8 < NiCo_8S_8 < Ni_3Co_6S_8$. Activity−properties correlations are discussed, on the basis of extended Hückel electronic structure calculations and temperature programmed reduction measurements.

Introduction

Periodic trends in the hydrodesulfurization (HDS) activity of transition metal sulfides (TMS) attract considerable attention of researchers. The correlations between structure and catalytic properties of sulfides are of key importance for elucidation of the reaction mechanism. They can also give some guidelines in the search for more active new sulfide phases. After the pioneering work of Pecoraro and Chianelli[1] concerning the catalytic properties of bulk metal sulfides in the dibenzothiophene HDS reaction, there were many other works dealing with bulk[2,3] and alumina[4] or carbon[5−11] supported sulfides in HDS[3−7] and other reactions such as hydrogenation[2,4] and hydrodenitrogenation.[8−11] Despite some minor differences, similar trends were found in all these works: (i) the sulfides of the 4d or 5d transition metals are much more active than those of the 3d metals, (ii) the maximum activity is observed for Ru and Rh along the second row and for Os and Ir along the third one. Originally, the latter trend was correlated with the enthalpy of formation of the sulfides taken as a measure of the metal−sulfur bond strength.[1] Since this approach did not explain the tendency observed for the 3d metals, it was modified using combinations of different parameters related to the electronic structure of the sulfides.[12−14] Thus, in a series of recent works, Raybaud et al. proposed to estimate the energies of the M−S bonds from the cohesion energy of the TMS.[15−18] The dependence of the HDS activity of bulk sulfides on such a "bond energy descriptor" has a volcano shape and obeys the well-known Sabatier principle: metal sulfides having optimal M−S bond energy (45−60 kcal/mol) exhibit high activities while both very low and very high energies result in poor activities.

It should be noted that only binary metal sulfides and Co(Ni)−MoS_2 or Co(Ni)−WS_2 combinations were included in such correlations as yet. Considering the ternary sulfides, a large class containing hundreds of compounds,[19] gives an opportunity to check the generality of structure−activity correlations on a larger basis. There are however some inherent experimental difficulties in realizing such a study. First, the HDS catalytic tests are performed in a hydrogen atmosphere at rather elevated temperatures (300−400 °C), conditions which impose a special demand on the materials' stability. Moreover, the ternary sulfides should be prepared in a highly dispersed form to allow correct measurement of their catalytic activity. As the methods of preparation of sulfides with high surface area are not well developed, special study of the preparation procedure is required. Up to now only one work dealing with the HDS properties of a series of ternary TMS sulfides, chromium thiospinels, has been reported.[20]

In this respect, the study of pentlandites can be of great interest. In a previous work we have found that mixed-cation pentlandites can be prepared in a highly dispersed form and are stable under a hydrogen atmosphere,[21] as required for study of HDS properties. Besides, a large number of compounds with various compositions can be obtained since in the pentlandite general formula M_9S_8, M can be Co (the only known binary pentlandite) or a mixture of Fe, Co, and Ni. Some heavy metals (Pd, Ag, Rh, Ru) can also enter the composition. In the structure of Co_9S_8 (space group *Fm*3*m*) the cobalt cations occupy one-eighth of the octahedral and one-half of the tetrahedral interstices within a nearly cubic close packing of sulfur.[22] The formula can thus be written as $[Co_{oct}][Co_{tetr}]_8S_8$, the tetracoordinated cations forming a cubic cluster $[Co_8S_6]$ with metal−metal bonds.[23] In mixed pentlandites, the Fe, Co, and Ni cations seem to be randomly distributed on the two crystallographic positions.[24] This class of sulfides thus offers a good opportunity for studying the catalytic properties for a series of compounds with the same structure and the same overall metal−sulfur stoichiometry.

In the present work we report the synthesis of highly dispersed binary and ternary pentlandites (Co_9S_8, $NiCo_8S_8$, $FeCo_8S_8$, $Ni_3Co_6S_8$, $Ni_{4.5}Fe_{4.5}S_8$), their characterization with special emphasis on the distribution of cations, and their catalytic properties in the thiophene hydrodesulfurization reaction.

* To whom correspondence should be addressed. Tel: +33 472 44 54 50. Fax: +33 472 44 53 99. E-mail: bezver@catalyse.cnrs.fr.
‡ E-mail: afanas@catalyse.cnrs.fr.
† E-mail: Michel.Danot@cnrs-imn.fr.

10.1021/jp049692u CCC: $27.50
Published on Web 05/07/2004

Experimental Section

Preparation of Pentlandites. The solids were prepared using reagent-grade metal salts from Sigma-Aldrich. After the final thermal treatment all sulfides were flashed with N_2 and stored in tightly closed bottles in order to prevent their oxidation.

Co_9S_8, $NiCo_8S_8$, $Ni_3Co_6S_8$. To prepare Co or Ni−Co mixed sulfides the metal nitrates $Co(NO_3)_2 \cdot 6H_2O$ and $Ni(NO_3)_2 \cdot 6H_2O$ were employed. Typically 0.01 mol of the salt or of the mixture of the salts was dissolved in 100 mL of water and a stoichiometric amount of $Na_2S \cdot 9H_2O$ dissolved in 100 mL of water was added dropwise under stirring. The dark precipitate formed was filtered, thoroughly washed with distilled water, and dried at room temperature under N_2 flow for 12 h. The precursor thus obtained was treated at 300 °C, under 15 vol % H_2S/H_2 mixture for 3 h and then under H_2 flow for the same time.

$FeCo_8S_8$. An 8.922 g (0.032 mol) amount of $CoSO_4 \cdot 7H_2O$ and 1.569 g (0.004 mol) of $(NH_4)_2Fe(SO_4)_2 \cdot 6H_2O$ were dissolved in 100 mL of water and to this mixture was quickly added a solution of 8.64 g (0.036 mol) of $Na_2S \cdot 9H_2O$ in 75 mL of water. Just after precipitation the solid was filtered, thoroughly washed with water, dried, and treated in the same fashion as the Co and Ni−Co sulfides.

$Ni_{4.5}Fe_{4.5}S_8$. We have observed that this Ni−Fe pentlandite cannot be prepared as a single phase through coprecipitation in aqueous solution. For this reason, we used a method similar to that proposed by Bouchard for synthesis of $Ni_xFe_{1-x}S_2$ solid solutions.[25] A 5.004 g (0.018 mol) amount of $FeSO_4 \cdot 7H_2O$ and 5.056 g (0.018 mol) of $NiSO_4 \cdot 7H_2O$ were dissolved in 60 mL of water. This solution was then added quickly to 500 mL of acetone under stirring. The mixed salt formed was first dried under N_2 at ambient temperature and then dehydrated at 100 °C under vacuum. The precursor was then treated at 350 °C under 50 vol % H_2S/N_2 flow for 6 h, then the temperature was decreased to 300 °C for the sample to be successively treated in 15 vol % H_2S/H_2 (3 h) and H_2 (3 h) flows.

Characterization. X-ray powder diffraction (XRD) patterns were recorded on a SIEMENS D5000 diffractometer using Cu Kα_1 radiation ($\lambda = 1.5406$ Å) with a 0.03° 2θ scan step. X-ray photoelectron spectra (XPS) were measured on a VG ESCALAB 200R device using Mg Kα radiation. Transmission electron microscopy (TEM) images were obtained on a JEOL 2010 microscope (point-to-point resolution 0.19 nm). The metal content in the synthesized solids was determined, after dissolution in a HNO_3/H_2SO_4 mixture, using plasma-coupled atomic emission spectroscopy (AES−ICP).

The EXAFS measurements were performed at the Laboratoire d'Utilisation du Rayonnement Electromagnétique (LURE, Orsay, France), on the XAS 13 spectrometer using a Ge (400) monochromator. The measurements were carried out in the transmission mode at the Fe K (7112 eV), Co K (7709 eV), and Ni K (8333 eV) edges at ambient temperature, with 2 eV step, 2 s per point. The sample thickness was chosen to give an absorption edge step of about 1.0 near the edge region (phase shift and backscattering amplitude were obtained from Co_9S_8). The EXAFS data were treated with VIPER[26] and FEFF[27] programs. The curve fitting was done in the R and k spaces. Coordination numbers (N), interatomic distances (R), Debye−Waller parameters (σ^2), and energy shifts (ΔE_0) were used as the fitting variables.

^{57}Fe Mössbauer measurements were performed in the transmission geometry, at room temperature, using a constant acceleration spectrometer equipped with a ^{57}Co(Rh) source (~20 mCi). The isomer shift reference is α-Fe (300 K).

TABLE 1: Lattice Parameters, Crystal Size, and Composition of the Pentlandites Prepared in the Work

sample	lattice parameter, Å	crystal size, Å		metal content, % calcd	metal content, % obsd
Co_9S_8	9.919	320	Co	67.4	66.8
$NiCo_8S_8$	9.932	380	Ni	7.5	7.3
			Co	59.9	58.9
$Ni_3Co_6S_8$	9.972	640	Ni	22.4	22.0
			Co	45.0	44.2
$FeCo_8S_8$	9.924	340	Fe	7.1	6.8
			Co	60.2	59.2
$Ni_{4.5}Fe_{4.5}S_8$	10.074	240	Ni	34.2	33.5
			Fe	32.6	31.8

Temperature programmed reduction (TPR) was carried out in a quartz reactor. The sulfide samples (ca. 0.01 g) were linearly heated (5 °C/min) up to 1000 °C under hydrogen flow. Hydrogen sulfide evolved during reduction was detected by a HNU photoionization detector equipped with a 10.2 eV UV light source. The amount of H_2S evolved was quantified after calibration of the detector with a gas mixture of known H_2S concentration.

Catalytic activities were measured for thiophene hydrodesulfurization at atmospheric pressure in a fixed-bed flow microreactor. The test conditions were chosen to provide a total thiophene conversion of less than 15%. The specific rate was determined after 15 h on stream at a pseudostationary state. BET surface areas of the solids before and after the test were calculated from a N_2 adsorption isotherm at 78 K.

Results and Discussion

Solid Characterization. Despite the mild conditions of the thermal treatment (300 °C), the XRD peaks of our sulfides are well-defined, even if broadened (see Supporting Information, Figure S1). The crystallite sizes, estimated from the line widths using the Scherrer equation, are characteristic of highly dispersed materials and depend somewhat on the composition (Table 1). All of the diffraction patterns can be ascribed to the pentlandite structure (for example, Co_9S_8, JCPD N65-1765). The lattice constants of our highly dispersed materials and their composition dependence (Table 1) are in fair agreement with what was previously reported for well-crystallized pentlandites prepared from the elements at high temperature.[24] It is worth noting that for $Ni_3Co_6S_8$, which was not reported earlier, the lattice parameter is consistent with the increase observed from Co_9S_8 to $NiCo_8S_8$, that is, for increasing Ni content.

The overall elemental compositions of the prepared solids (Table 1) correspond well to the calculated ones. Along with the XRD data this allows one to conclude that the developed preparation procedures lead to single-phase mixed pentlandites. An important point is, however, the homogeneity of the metal distribution at the microscopic scale. It should be reminded that the only stable binary pentlandite is Co_9S_8, which excludes the possibility for the Fe−Co and Ni−Co mixed sulfides to be mixtures of two binary pentlandites. However, some nonuniformity in the element distribution within the homogeneity range of the pentlandite structure cannot be excluded. To sort out this point, high-resolution electron microscopy with local EDX analysis was used. Even for the smallest size of the EDX spot (analyzed surface ~15 nm^2) the composition of all of our mixed compounds appears rather constant and very close to the overall stoichiometry (the results of some local analysis are presented in Figure 1 for $NiCo_8S_8$ and $Ni_{4.5}Fe_{4.5}S_8$). This means that the ternary sulfides under study are homogeneous solids, at least at the analysis scale.

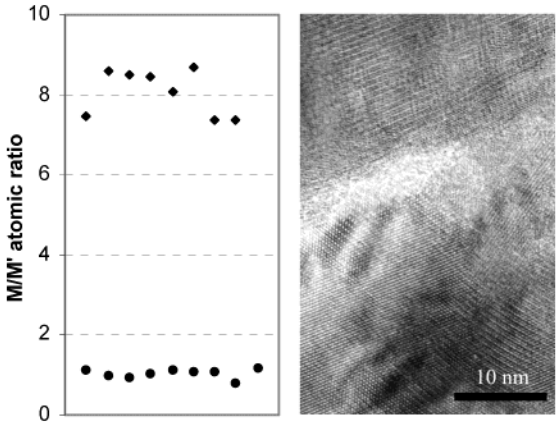

Figure 1. HRTEM image of $Ni_{4.5}Fe_{4.5}S_8$ particle and local composition of $NiCo_8S_8$ (squares) and $Ni_{4.5}Fe_{4.5}S_8$ (circles) by EDX analysis (15 nm^2 spot diameter).

Another question concerns the cation distribution on the two different crystallographic sites. To resolve this problem we carried out an EXAFS study of our mixed pentlandites in order to compare the coordination shells of the different cations. The EXAFS spectra have been recorded at each of the cation K-edges for $NiCo_8S_8$, $Ni_3Co_6S_8$, $FeCo_8S_8$, and $Fe_{4.5}Ni_{4.5}S_8$, as well as at the Co K-edge for Co_9S_8. The corresponding Fourier transformation (FT) curves are presented in Figure 2. Most of the FTs show a first enlarged peak typical of the pentlandite structure for which it corresponds to several types of sulfur neighbors along with close-standing cations (ca 2.5 Å).

In the case of Co_9S_8, EXAFS data fitting is rather difficult because, since their atomic numbers differ by a factor of about 2, cobalt and sulfur have nearly opposite scattering phases (the same is true for Ni/S and Fe/S). Due to this phase opposition and the similarity of several Co−S and Co−Co distances in the pentlandite structure, contributions from Co and S neighbor shells may become mutually extinct which results in important uncertainty in the fitting procedure. Fortunately, the XRD study unambiguously shows the pentlandite structure of our Co_9S_8 sample (and of all our mixed sulfides as well) which allows some constraints on the distances to be introduced. In these conditions, we obtained a satisfactory fit in both k and R spaces for Co_9S_8, using 11 coordination shells. The complete fit results are given in the Supporting Information (Tables S1 and S2) and the experimental and calculated FTs presented in Figure 2a. The variable parameters refine to values close to those calculated from the crystalline structure. Note for example the number of sulfur neighbors at 2.39 Å in the CoS_6 octahedral sites which refines to 0.5 ($N = 6/9$ according to the crystalline structure), or the number of Co next-nearest neighbors in the cubic cluster, lying on the diagonal plane ($d = 3.51$ Å), which refines to $N = 3.4$ ($N = 3$ according to the crystalline structure). This level of accuracy seems sufficient to allow eventual site preference of the cations involved in our mixed phases to be detected, especially for the solids where 1/9 of the cobalt atoms is substituted (in this case the substituent could occupy only the octahedral positions leaving the tetrahedral sites to cobalt).

The data relative to the substituted solids were processed using the interatomic distances, Debye−Waller factors, and energy shifts obtained for Co_9S_8 as fixed parameters. Only the coordination numbers were refined. Such a procedure is of course an approximation, but it provides a compromise between physical rigor and calculation difficulty.

No significant difference can be observed between the FTs obtained at the Ni and Fe K-edges for $Fe_{4.5}Ni_{4.5}S_8$ (Figure 2b).

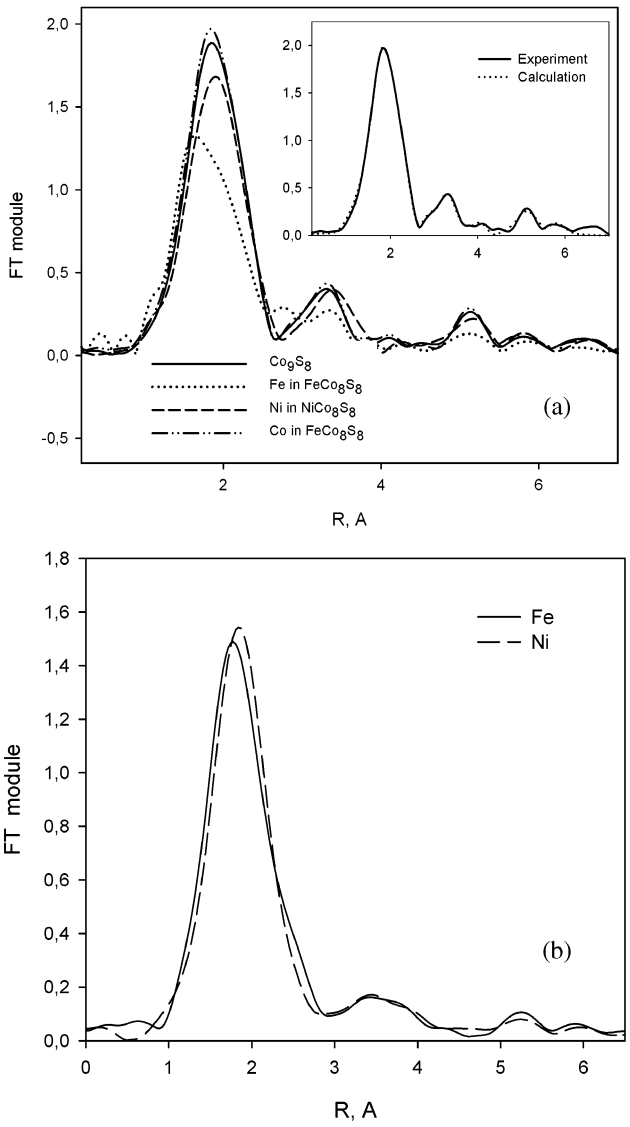

Figure 2. FT of EXAFS spectra of the pentlandites: (a) Co_9S_8, $NiCo_8S_8$, and $FeCo_8S_8$ (insert: Co K-edge in comparison with the theoretical fit), (b) Fe and Ni K-edge spectra of $Ni_{4.5}Fe_{4.5}S_8$.

Consistently, the coordination numbers refined for both Ni and Fe are similar, and close by those of Co in Co_9S_8. This allows one to conclude that nickel and iron are randomly distributed between the T_d and O_h sites, within the limits of the method accuracy. Similar FTs were obtained as well for Ni and Co in $NiCo_8S_8$ (Figure 2a), which also points to random distribution of the two cations. By contrast, in the case of $FeCo_8S_8$, an important difference between the Fe and Co FTs is observed (Figure 2a): for Co, the FT is similar to that in Co_9S_8, for Fe, the first peak is less symmetrical and located at a smaller distance than for Co. Detailed analysis shows that this is related to a greater number of sulfur neighbors at 2.39 Å and a smaller number of cation neighbors at 2.50 Å for Fe than for Co. Both of these results show that iron prefers an octahedral environment. Effectively, according to the refined coordination numbers, about one-half of the iron atoms are located in octahedral sites, instead of 1/9 for random distribution. In these conditions, cobalt obviously cannot be randomly distributed in $FeCo_8S_8$. However, the fact that its FT is similar to that in Co_9S_8 is not surprising because the cobalt EXAFS signal is mainly related to the tetrahedral sites whose population is not perturbed a lot by the iron site preference, due to the small overall iron amount.

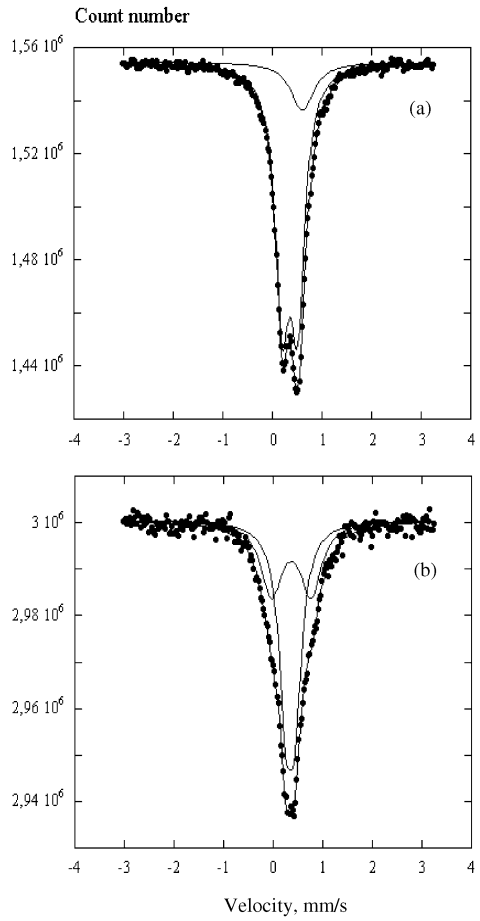

Figure 3. ^{57}Fe Mössbauer spectra of (a) $Ni_{4.5}Fe_{4.5}S_8$ and (b) $FeCo_8S_8$ (room temperature, chemical shifts are relative to α-Fe).

In the case of the Fe-containing pentlandites the conclusions about cation distribution based on the EXAFS data were additionally confirmed by ^{57}Fe transmission Mössbauer spectroscopy. The spectrum of $Ni_{4.5}Fe_{4.5}S_8$ (Figure 3a) can be described considering a doublet (1) on a broadened single line (2) with the following parameters (δ, isomer shift; Δ, quadruple splitting; Γ, full width at half-height; A, spectral contribution):

$$\delta_1 = 0.36 \text{ mm/s}, \Delta_1 = 0.31 \text{ mm/s}, \Gamma_1 = 0.34 \text{ mm/s}, A_1 = 86\%$$

$$\delta_2 = 0.61 \text{ mm/s}, \Gamma_2 = 0.55 \text{ mm/s}, A_2 = 14\%$$

The parameters observed are close to those previously reported for well-crystallized materials.[24] The ratio of the spectral contributions corresponding to the iron atoms in tetrahedral (doublet) and octahedral (single line) positions ($T_d/O_h = 6.1$) is close by the ideal value ($T_d/O_h = 8$), which means that in $Ni_{4.5}Fe_{4.5}S_8$ iron, and consequently nickel, randomly occupy the two cationic positions.

The Mössbauer spectrum of $FeCo_8S_8$ (Figure 3b) somewhat differs from that of $Ni_{4.5}Fe_{4.5}S_8$ (Figure 3a). It can also be described with two components, two quadruple doublets:

$$\delta_1 = 0.36 \text{ mm/s}, \Delta_1 = 0.80 \text{ mm/s}, \Gamma_1 = 0.50 \text{ mm/s}, A_1 = 40\%$$

$$\delta_2 = 0.35 \text{ mm/s}, \Delta_2 = 0.18 \text{ mm/s}, \Gamma_2 = 0.34 \text{ mm/s}, A_2 = 60\%$$

TABLE 2: Results of the Extended Hückel Calculations

sample	cohesion energy $-\Delta E$, kcal/$P1$ unit cell	Fermi energy $-E_f$, eV
Co_9S_8	573	11.43
$NiCo_8S_8$	571	11.30
$Ni_3Co_6S_8$	548	10.95
$Ni_{4.5}Fe_{4.5}S_8$	551[a]	11.02[a]
	556[b]	11.08[b]

[a] Random Fe distribution. [b] Fe located in the octahedra.

It is difficult in this case to unambiguously decide which of these components corresponds to the octahedral sites and which to the tetrahedral ones. However, since the ratio of the spectral contributions is close to unity, it can be deduced that about half of the iron atoms are located in the octahedra, in good agreement with the EXAFS results. It should be noted that in the case of $FeCo_8S_8$ the parameters of the spectral components are slightly different from those reported earlier.[24] We suggest that this effect is due to differences in the iron distributions on the two crystallographic positions. In the solids prepared at high temperature from the elements, the spectral contribution ratio was found equal to 6[24]. This means that the Fe atoms occupy almost randomly the T_d and O_h positions while in our sample there are many fewer Fe atoms in the tetrahedra. Such a change in the composition of the metal clusters formed by the tetrahedrally coordinated atoms can modify the electronic structure of the clusters and consequently the Mössbauer parameters of Fe which are sensitive even to slight changes in the electron distribution.

Electronic Structure. Burdett and Miller studied the electronic structure of Co_9S_8 using extended Hückel (EH) calculations. They evidenced a significant delocalization of the cobalt d orbitals and strong interactions between the metal atoms in the tetrahedral positions,[23] resulting in broad bands consistent with the metallic properties of pentlandites (metallic conductivity and luster or Pauli paramagnetism).

We repeated the calculations of Burdett and Miller for Co_9S_8 and performed EH calculations for our substituted phases in order to compare the stabilization energies and to illustrate qualitatively the bonding changes within the series (despite its low absolute precision, the EH method allows one to follow the qualitative trends of chemical bonding in solids). The Fermi energy (E_f) and cohesion energy (ΔE, for the reduced unit cell with $P1$ symmetry) values are summarized in Table 2 for our different pentlandites.

To check to what extent E_f and ΔE depend on the cation distribution on the octahedral and tetrahedral sites, we performed two calculations for $Ni_{4.5}Fe_{4.5}S_8$, one with random distribution of Fe and Ni, the other with all the O_h sites occupied by Fe. It appears that the results are almost identical whatever the cation distribution (Table 2). For the whole series of materials (Table 2) the differences in cohesion energy are low, less than 30 kcal/mol per unit cell, that is, less than 1 kcal per sulfur atom (the $P1$ reduced unit cell contains 32 sulfur atoms). The Fermi levels range from −10.90 to −11.43 eV. The value we found for Co_9S_8 ($E_f = -11.43$ eV) is close to that reported by Burdett and Miller (−11.49 eV). It is the smallest value of the whole series. Replacement of Co by Fe or Ni leads to a change in the d-electron count. Simultaneously, band shift occurs because of the different charges of the nuclei. Along the sequence Fe−Co−Ni these two effects have opposite signs and the resulting change in the Fermi energy is not very important. As follows from consideration of the DOS projections of the d orbitals of the different cations, the variations of the Fermi levels and band positions do not lead to any qualitative change of bonding in

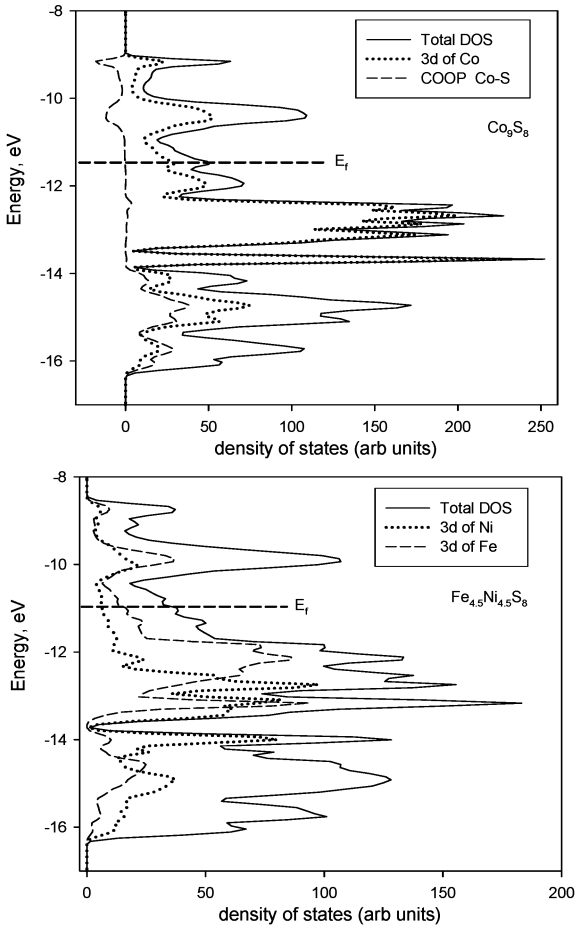

Figure 4. Density of states diagrams (DOS) derived from extended Hückel calculations for Co_9S_8 (top) and $Ni_{4.5}Fe_{4.5}S_8$ (bottom).

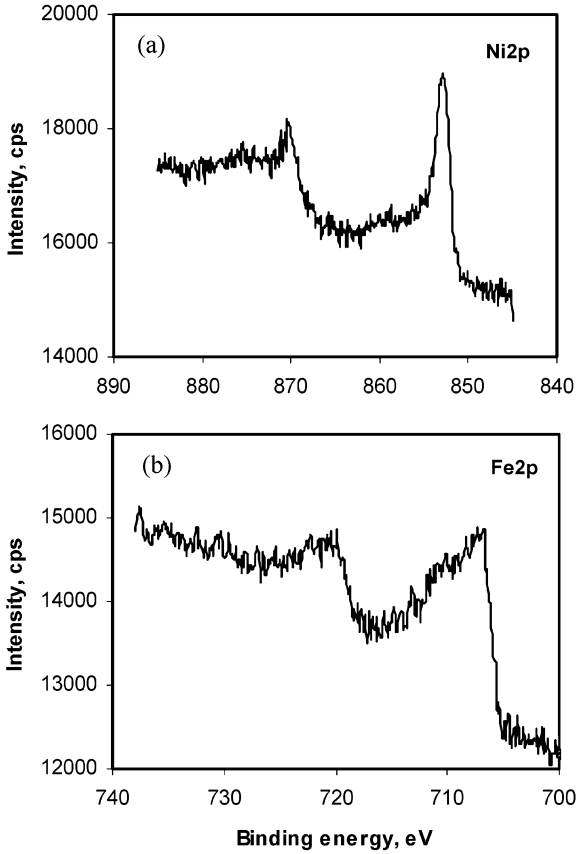

Figure 5. Ni(2p) (a) and Fe(2p) XPS spectra (b) of $Ni_{4.5}Fe_{4.5}S_8$.

these solids (Figure 4). The orbitals at the Fermi level (HOMO) are mostly derived from the d_{xy} and d_{yz} orbitals of the cations in tetrahedral coordination, whereas the d orbitals of the octahedrally coordinated cations are much more localized. This is true for all the solids studied, within the range of the observed E_f variations. The metal−sulfur antibonding levels of the M_8S_6 cubic cluster remain unoccupied in all cases. The borderline between the bonding and antibonding M−S orbitals lies near E_f, a region where the total overlap population is rather low. At the same time, the M−M interactions have a strong share of antibonding character. Concerning the band positions, as expected the d-orbital energy is found lower for nickel than for iron, which is consistent with the mostly Fe character of the HOMO levels (Figure 4).

Catalytic Properties. The catalytic properties of our pentlandites in the thiophene HDS reaction are summarized in Table 3. The composition of the products of thiophene transformation on the pentlandites differs significantly from that found previously on the MoS_2-based catalysts. A considerably higher butenes/butane ratio (up to 130, instead of ca. 2 for MoS_2) means that ternary pentlandites, as other 3d metal sulfides,[2] have a poor hydrogenation activity compared to that of sulfides of 4d and 5d metals. The reaction rates in Table 3 are expressed as specific activities, A_S (per mass unit of the catalyst), and intrinsic activities, A_i (per surface unit of the solid after reaction). In our case all the solids have the same cubic structure, which is highly isotropic. Therefore, we consider that using the A_i values, directly related to the number of the surface atoms, is more pertinent for comparison of the catalytic activities.

The catalytic activity of our pentlandites is sensitive even to a slight composition change; replacement of only one out of nine Co atoms by Fe significantly decreases the activity. Extremely low activity is observed for $Ni_{4.5}Fe_{4.5}S_8$ (Table 3). Considering the largely better activity of Co_9S_8, this result can be found surprising since these two compounds are isoelectronic, with only a slight difference between their lattice parameters (10.074 Å for $Ni_{4.5}Fe_{4.5}S_8$, 9.919 Å for Co_9S_8). As we have shown above, the particles' composition is uniform, at least at the 15 nm^2 scale, and the Ni and Fe cations randomly occupy the octahedral and tetrahedral sites. It cannot be excluded, however, that one of the elements (presumably Fe) is segregated on the surface leading to the drastic drop of activity. To check this possibility we studied the surface composition using X-ray photoelectron spectroscopy (Figure 5). The observed binding

TABLE 3: Textural and Catalytic Properties of the Studied Pentlandites and Their Reducibility

sample	S_{BET}, m^2/g		rate of thiophene HDS at 300 °C		butenes/butane ratio	maxima in TPR patterns, °C
	before test	after test	A_S, 10^{-8} mol/(g s)	A_i, 10^{-8} mol/(m^2 s)		
Co_9S_8	50.4	40.0	40	1.0	69	680
$NiCo_8S_8$	29.4	26.4	28	1.1	41	675
$Ni_3Co_6S_8$	12.7	12.8	17	1.3	133	670
$FeCo_8S_8$	36.0	33.0	21	0.6	123	688
$Ni_{4.5}Fe_{4.5}S_8$	38.5	36.2	1	0.03	110	619, 714

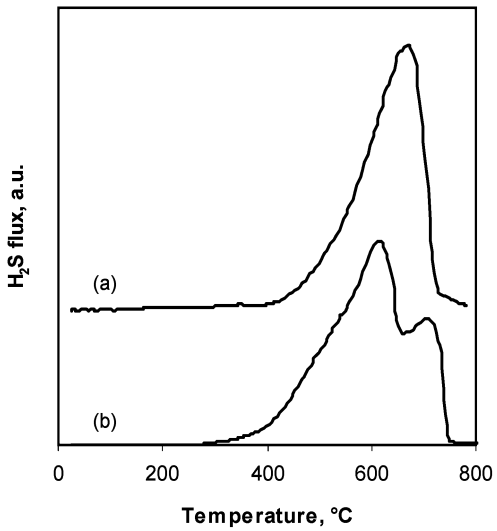

Figure 6. Temperature programmed reduction patterns for (a) Co_9S_8 and (b) $Ni_{4.5}Fe_{4.5}S_8$.

energies of Ni ($2p_{3/2}$) (E_b = 852.9 eV) and Fe ($2p_{3/2}$) (E_b = 707.1 eV) are typical for these cations in a sulfur environment.[28−30] The asymmetry of the broad Fe 2p peak possibly reflects the formation of various oxysulfide environments due to partial oxidation during the transfer of the sulfide to the UHV chamber of the XPS spectrometer. Such a tail in the higher energy range is frequently observed in the XPS spectra of iron in sulfides.[30] The Ni/Fe ratio on the surface, deduced from the peak areas corrected with theoretical cross-sections,[31] is 0.92, which is very close to the value determined from the chemical analysis (Table 1). It means that the surface composition of $Ni_{4.5}Fe_{4.5}S_8$ is the same as in the bulk and that the low catalytic activity observed is a characteristic related to the very nature of this compound and not to some deviations in the uniformity of the cation distribution.

The very low catalytic activity of $Ni_{4.5}Fe_{4.5}S_8$ can be correlated to its particular behavior in temperature programmed reduction (TPR) (Figure 6). The TPR profiles of all our other (Co-containing) pentlandites are very similar with a unique reduction step and close values of the peak maximum temperatures (Table 3). On the contrary, $Ni_{4.5}Fe_{4.5}S_8$ reduces in two stages, the first peak being located at 619 °C. That is, significantly lower than the unique peak of our other pentlandites (~680 °C). The fact that $Ni_{4.5}Fe_{4.5}S_8$ begins to reduce at about 60 °C lower than our Co-containing pentlandites indicates that its reduction mechanism is different and that at least part of its sulfur atoms have a significantly lower bonding energy.

Concerning the applicability of the Sabatier principle to mixed sulfides, we tried to correlate the observed catalytic activities of our pentlandites with the average metal−sulfur bond strengths derived from the experimental cohesion energies of Co_9S_8, Ni_3S_2, and FeS[16] (Table 4). The material having the lowest metal−sulfur bond energy, $Ni_{4.5}Fe_{4.5}S_8$, is the least active one, which means that catalytic activity of our pentlandites decreases with metal-sulfur bond strength in accordance with the Sabatier principle. It could seem surprising that a relatively small variation in bonding energy (7 kcal/mol) leads to such a significant change in the catalytic activity. However, the theoretical difference in activity (estimated, for example, from the curve in Toulhoat's work[16]) for the given values of metal−sulfur bond strengths is about 1 order of magnitude and thus not very far from the difference observed here, taking into account that experimental error is more important when measuring the very low activities.

TABLE 4: Average Metal−Sulfur Bond Strengths and Catalytic Properties of the Studied Pentlandites

sample	average M−S bond strength,[a] kcal/mol	A_i (300 °C), 10^{-8} mol/(m^2 s)
Co_9S_8	43.6	1.0
$NiCo_8S_8$	43.4	1.1
$Ni_3Co_6S_8$	42.9	1.3
$FeCo_8S_8$	42.3	0.6
$Ni_{4.5}Fe_{4.5}S_8$	36.6	0.03

[a] Average values are calculated from M−S bonding energies for Co_9S_8, Ni_3S_2 (41.3 kcal/ mol), and FeS (31.8 kcal/mol) given by Toulhoat et al. (16).

Accounting for the general tendency, the average M−S bond energy fails however to explain more subtle variations in observed activities. Thus, $Ni_3Co_6S_8$ and $FeCo_8S_8$ have nearly the same bond energies and similar TPR patterns, but their catalytic activities differ by a factor of 2. This discrepancy can be due to the fact that in the case of $FeCo_8S_8$ formation of surface sulfur vacancies coordinated by iron neighbor is favored. Indeed, as the Fe−S bond is weaker than the Co−S one, the surface sulfur atoms having mixed cation surrounding will be eliminated more easily than those bounded only to Co. So, the share of "mixed cation vacancies" at the surface will be higher than statistically expected from the overall high Co/Fe ratio. The quality of these vacancies as active centers in HDS reaction is poor, precisely due to a weak sulfur bonding, and the activity of $FeCo_8S_8$ is thus significantly lower than anticipated on the basis of the iron content.

Supporting Information Available: XRD patterns of the pentlandites studied in the work, tables containing the complete lists of structural parameters derived from EXAFS spectra of Co_9S_8 and $FeCo_8S_8$ (Fe K-edge). This material is available free of charge via the Internet at http://pubs.acs.org.

References and Notes

(1) Pecoraro, T. A.; Chianelli, R. R. *J. Catal.* **1981**, *67*, 430.
(2) Lacroix, M.; Boutarfa, N.; Guillard, C.; Vrinat, M.; Breysse, M. *J. Catal.* **1989**, *120*, 473.
(3) Hermann, N.; Brorson, M.; Topsoe, H. *Catal. Lett*. **2000**, *65*, 169.
(4) Quartararo, J.; Mignard, S.; Kasztelan, S. *J. Catal*. **2000**, *192*, 307.
(5) Hensen, E. J. M.; Brans, H. J. A.; Lardinois, G. M. H. J.; de Beer, V. H. J.; van Veen, J. A. R.; van Santen, R. A. *J. Catal*. **2000**, *192*, 98.
(6) Vissers, J. P. R.; Groot, C. K.; van Oers, E. M.; de Beer, V. H. J.; Prins, R. *Bull. Soc. Chim. Belg*. **1984**, *93*, 813.
(7) Ledoux, M. J.; Michaux, O.; Agostini, G.; Panissod, P. *J. Catal.* **1986**, *102*, 275.
(8) Eijsbouts, S.; de Beer, V. H. J.; Prins, R. *J. Catal.* **1988**, *109*, 217.
(9) Ledoux, M. J.; Djellouli, B. *J. Catal*. **1989**, *115*, 580.
(10) Eijsbouts, S.; Sudhakar, C.; de Beer, V. H. J.; Prins, R. *J. Catal.* **1991**, *127*, 605.
(11) Eijsbouts, S.; de Beer, V. H. J.; Prins, R. *J. Catal.* **1991**, *127*, 619.
(12) Harris, S.; Chianelli, R. R. *J. Catal*. **1984**, *86*, 400.
(13) Harris, S.; Chianelli, R. R. *Chem. Phys. Lett.* **1983**, *101* (6), 603.
(14) Smit, T. S.; Johnson, K. H. *Catal. Lett.* **1994**, *28*, 361
(15) Raybaud, P.; Kresse, G.; Hafner, J.; Toulhoat, H. *J. Phys.: Condens. Matter* **1997**, *9*, 11085.
(16) Toulhoat, H.; Raybaud, P.; Kasztelan, S.; Kresse, G.; Hafner, J. *Catal. Today* **1999**, *50*, 629.
(17) Toulhoat, H.; Raybaud, P J. *J. Catal*. **2003**, *216*, 63.
(18) Chianelli, R. R.; Berhault, G.; Raybaud, P.; Kasztelan, S.; Hafner, J.; Toulhoat, H. *Appl. Catal. A* **2002**, *227*, 83.
(19) Jelinek, F. Sulphides. In *Inorganic Sulfur Chemistry*; Nickless, G., Ed.; Elsevier: New York, 1968.
(20) Thiollier, A.; Afanasiev, P.; Delichere, P.; Vrinat, M. *J. Catal.* **2001**, *197*, 58.
(21) Bezverkhyy, I.; Danot, M.; Afanasiev, P. *Inorg. Chem.* **2003**, *42*, 1764.
(22) Rajamani, V.; Prewitt C. T. *Can. Mineral.* **1975**, *13*, 75.
(23) Burdett, J. K.; Miller G. J. *J. Am. Chem. Soc.* **1987**, *109*, 4081.

(24) Knop, O.; Huang, C.-H.; Reid, K. I. G.; Carlow, J. S.; Woodhams F. W. D. *J. Solid State Chem.* **1976**, *16*, 97.
(25) Bouchard R. J. *Mater. Res. Bull.* **1968**, *3*, 563.
(26) Klementiev, K. V. *VIPER for Windows*, freeware: www.desy.de/~klmn/ viper.html. Klementiev, K. V. *J. Phys. D: Appl. Phys.* **2001**, *34*, 209.
(27) Rehr, J. J.; Zabinsky S. I.; Albers, R. C. *Phys. Rev. Lett.* **1992**, *69*, 3397.
(28) Pratt A. R.; Nesbitt H. W.; Muir, I. J. *Geochim. Cosmochim. Acta* **1994**, *58*, 827.
(29) *Handbook of Photoelectron Spectroscopy*; Chastain, J., Ed.; Perkin-Elmer Corporation: Eden Prairie, MN, 1992.
(30) Mullet, M.; Boursiquot S.; Abdelmoula M.; Génin J.-M.; Ehrhardt J.-J. *Geochim. Cosmochim. Acta* **2002**, *66*, 829.
(31) Scofield, J. H. *Electron. Spectrosc. Related Phenom.* **1976**, *8*, 129.